

RAMPED-INDUCED STATES IN THE PARAMETRICALLY DRIVEN GINZBURG-LANDAU MODEL

Boris A. Malomed

Department of Interdisciplinary Studies, Faculty of Engineering, Tel Aviv
University, Tel Aviv 69978, Israel

Horacio G. Rotstein

Department of Chemistry and Volen Center for Complex Systems, Brandeis
University, MS 015 Waltham, MA 02454-9110, USA

Abstract

We introduce a parametrically driven Ginzburg-Landau (GL) model, which admits a gradient representation, and is subcritical in the absence of the parametric drive (PD). In the case when PD acts uniformly in space, this model has a stable kink solution. A nontrivial situation takes place when PD is itself subject to a kink-like spatial modulation, so that it selects real and imaginary constant solutions at $x = \pm\infty$. In this situation, we find stationary solutions numerically, and also analytically for a particular case. They seem to be of two different types, viz., a pair of kinks in the real and imaginary components, or the same with an extra kink inserted into each component, but we show that both belong to a single continuous family of solutions. The family is parametrized by the coordinate of a point at which the extra kinks are inserted. However, solutions with more than one kink inserted into each component do not exist. Simulations show that the former solution is always stable, and the latter one is, in a certain sense, neutrally stable, as there is a special type of small perturbations that remain virtually constant in time, rather than decaying or growing (they eventually decay, but extremely slowly).

1 Introduction

Various forms of parametrically driven Ginzburg-Landau (GL) equations constitute a class of pattern-forming systems with broken intrinsic phase-rotation invariance [1, 2]. In this work, we consider a *gradient* model of this type,

$$u_t = \epsilon(x) \cdot u^* + \zeta u + u_{xx} - |u|^2 u \equiv -\frac{\delta L}{\delta u^*}, \quad (1)$$

where u^* stands for the complex conjugation, $\delta/\delta u^*$ is the variational derivative, the function $\epsilon(x)$ and constant ζ are real, and the *Lyapunov functional* is

$$L = \frac{1}{2} \int_{-\infty}^{+\infty} [-\epsilon(x) \cdot (u^2 + (u^*)^2) - \zeta |u|^2 + |u_x|^2 + |u|^4] dx. \quad (2)$$

Equation (1) with $\epsilon = \text{const}$ has various applications, the best-known one being the Rayleigh-Bénard convection in the case when the convection-driving temperature difference across the fluid layer is subject to a resonant periodic modulation along the layer (the coordinate x is running along the layer), or the boundary is similarly undulated, see early [3] and more recent [4] theoretical works on this topic, and an experimental work [5]. The “resonant” character of the modulation means that its period is half the depth of the convective layer. The presence of the variable coefficient $\epsilon(x)$ implies that the “primary” modulation is further subject to a “supermodulation” on a scale essentially larger than the layer’s depth, which is quite possible in large-aspect-ratio convection cells, and gives rise to novel patterns, as it will be shown below.

The real constant ζ in Eq. (1) controls the system’s overcriticality in the absence of the parametric drive: when $\epsilon = 0$, the situation is *overcritical* if $\zeta > 0$, and *subcritical* if $\zeta < 0$. Rescaling allows one to reduce ζ to one of the three values, $\zeta = -1, 0$, or $+1$. To the best of our knowledge, the previous works were dealing with the case when the gradient GL system was overcritical when $\epsilon = 0$. Our aim is to consider the opposite case with $\zeta = -1$, when no nontrivial pattern may exist without the parametric drive. Thus, $\zeta \equiv -1$ will be assumed below, unless another value of ζ is specified.

In the case $\epsilon = \text{const}$, Eq. (1) has obvious constant solutions,

$$u_0 = \pm\sqrt{\epsilon - 1}, \text{ or } u_0 = \pm i\sqrt{-\epsilon - 1}, \quad (3)$$

which exist provided that, respectively, $\epsilon > 1$ or $\epsilon < -1$, while the trivial solution $u = 0$ is stable in the case $|\epsilon| \leq 1$, when the nonzero solutions (3) do not exist. In the case $|\epsilon| > 1$, another available exact solution is a *kink*, or domain wall, which provides for a transition between the constant solutions (3) with the opposite signs. For instance, in the case $\epsilon > 1$ (recall we set $\zeta = -1$), the kink solution to Eq. (1) is

$$u_{\text{kink}}(x) = \sigma \sqrt{\epsilon - 1} \tanh \left(x \sqrt{\frac{\epsilon - 1}{2}} \right), \quad (4)$$

where $\sigma = \pm 1$ is the kink's polarity.

Note that a similar kink, with $(\epsilon - 1)$ replaced by 1 is, simultaneously, an exact solution to the usual GL equation, which can be obtained from Eq. (1) setting $\epsilon = 0$ and $\zeta = +1$. It is commonly known that, in its latter capacity, the real kink solution is unstable against purely imaginary perturbations. On the contrary to this, an elementary consideration demonstrates that the solution (4) is stable as a solution to the parametrically driven GL equation (1) with $\zeta = -1$ and $\epsilon > 1$. This is a formally new result, but the actual objective of the work is to consider more interesting solutions in the case when the parametric drive is *ramped*, i.e., it is itself subject to a kink-like modulation, see below.

2 The ramp and stationary solutions

A configuration with $\epsilon(x)$ monotonically varying between asymptotically constant values at $x = \pm\infty$ is called a *ramp*. In the case of the usual (not parametrically driven) GL equation, much work has been done for a case when the overcriticality is ramped so that the system is subcritical at $x = -\infty$ and supercritical at $x = +\infty$, as this configuration makes it possible to uniquely solve the *wavenumber-selection problem*, and demonstrates other remarkable features [7]. Moreover, the ramp problem can be extended into the two-dimensional geometry, replacing u_{xx} by the two-dimensional Laplacian. In particular, the stability of the ramp-supported quasi-one-dimensional pattern in the two-dimensional version of the usual GL equations was investigated in Refs. [6]. In the parametrically driven equation (1) with $\zeta = -1$, a similar ramp can easily be arranged too, choosing a function $\epsilon(x)$ which is monotonically varying between a value $|\epsilon(-\infty)| < 1$, that provides for the stability of

the $u = 0$ solution at $x = -\infty$, and $|\epsilon(+\infty)| > 1$, which gives rise to a stable nonzero solution (3) at $x = +\infty$.

The subject of this work is to consider a more nontrivial case of the ramp, when $\epsilon(x)$ interpolates between values $\epsilon(-\infty) < -1$ and $\epsilon(+\infty) > +1$, for instance

$$\epsilon(x) = a \tanh(\lambda x), \quad a > 1, \quad \lambda > 0. \quad (5)$$

This ramp supports purely imaginary and purely real nonzero states (3) at $x = -\infty$ and $x = +\infty$, so that $u(x = -\infty) = \pm i\sqrt{a-1}$, $u(x = +\infty) = \pm\sqrt{a-1}$. Our objective is to find solutions interpolating between these asymptotic states, and investigate their stability. A configuration of the present type can be easily implemented experimentally, which makes the problem physically relevant (in the convective layer, the constant imaginary and real solutions represent uniform arrays of convection rolls mutually shifted by half the layer's depth).

For the numerical solution of Eq. (1) with $\zeta = -1$ and $\epsilon(x)$ taken as per Eq. (5), we define $u(x) \equiv v(x) + iw(x)$, arriving at a system of equations for two real functions,

$$v_t = a \tanh(\lambda x) \cdot v + v_{xx} - (v^2 + w^2 + 1)v = 0, \quad (6)$$

$$w_t = -a \tanh(\lambda x) \cdot w + w_{xx} - (v^2 + w^2 + 1)w = 0. \quad (7)$$

Boundary conditions (b.c.) corresponding to the situation defined above are

$$v(x = -\infty) = 0, \quad v(x = +\infty) = \pm\sqrt{a-1}, \quad (8)$$

$$w(x = -\infty) = \pm\sqrt{a-1}, \quad w(x = +\infty) = 0, \quad (9)$$

the signs \pm in Eqs. (8) and (9) being mutually independent. Obvious symmetries of the equations allow us to fix only one set of the signs, as solutions corresponding to other combinations of the signs are actually the same.

Getting back for a moment to Eq. (1) with $\zeta = +1$, it is worthy to note that, in this case, a particular choice $a = 1$ and $\lambda = 1/\sqrt{2}$ gives rise to an *exact* stationary solution interpolating between the real and imaginary asymptotic states, viz.,

$$v(x) = (1/\sqrt{2}) [1 + \tanh(x/\sqrt{2})], \quad w(x) = (1/\sqrt{2}) [1 - \tanh(x/\sqrt{2})]. \quad (10)$$

However, if $\zeta = -1$, no similar exact solution can be found. There is only one analytically tractable (and rather unphysical) case, which is $\lambda \ll 1$, i.e., a very broad ramp. In this case, defining $\xi \equiv \lambda x$, one can readily see that the x -derivative terms in Eqs. (6) and (7) are negligible, and an asymptotically exact stationary solution corresponding to $\lambda \rightarrow 0$ is

$$\begin{aligned} w &= 0, \quad v^2 = a \tanh \xi - 1 \quad \text{at} \quad \tanh \xi > 1/a, \\ v &= 0, \quad w^2 = -a \tanh \xi - 1 \quad \text{at} \quad \tanh \xi < -1/a, \\ v &= w = 0 \quad \text{at} \quad |\tanh \xi| < 1/a. \end{aligned} \quad (11)$$

Of course, at small but finite λ the fields which exactly vanish in various regions in the limit $\lambda = 0$ have small nonzero values at all ξ .

In order to understand the structure of solutions to Eqs. (6) and (7), we consider the following auxiliary system,

$$\begin{cases} v_{xx} - (\alpha^2 v^2 + \alpha^2 w^2 + 1) v + a g(x)v = 0, \\ w_{xx} - (\alpha^2 v^2 + \alpha^2 w^2 + 1) w - a g(x)w = 0, \end{cases} \quad (12)$$

subject to b.c.

$$\begin{cases} v(-\infty) = 0, & v(\infty) = 1, \\ w(-\infty) = 1, & w(\infty) = 0. \end{cases} \quad (13)$$

Here $\alpha = \sqrt{a-1}$, and

$$g(x) \equiv \begin{cases} 1, & x \in [\eta, \infty) \\ x/\eta, & x \in [-\eta, \eta] \\ -1, & x \in (-\infty, -\eta] \end{cases}, \quad (14)$$

with $0 < \eta \ll 1$. The system (12) reduces to Eqs. (6)-(7) if one substitutes $g(x)$ by $\tanh(\lambda x)$, simultaneously replacing v and w by v/α and w/α in Eqs. (6)-(7).

It is easy to see that, due to symmetry arguments, $v(x) = w(-x)$ and $v(-x) = w(x)$, which in particular means that $v(0) = w(0)$. Far from the origin, obvious *outer-zone* solutions to Eqs. (12) satisfying b.c. (13) are

$$\begin{cases} v = \pm 1, \quad w = 0, & \text{at} \quad x \geq \eta, \\ v = 0, \quad w = \pm 1, & \text{at} \quad x \leq -\eta. \end{cases} \quad (15)$$

Inside the interval $x \in [-\eta, \eta]$ one has, to the leading order in the small parameter η , $v_{xx} = w_{xx} = 0$. An *inner-zone* solution to these equations, satisfying b.c. $v(\eta) = 1$, $v(-\eta) = 0$, $w(\eta) = 0$ and $w(-\eta) = 1$, which are necessary for the continuous matching to the outer-zone solution (15) with the upper sign, is

$$v = \frac{x}{2\eta} + \frac{1}{2}, \quad w = -\frac{x}{2\eta} + \frac{1}{2}. \quad (16)$$

Thus, to the leading order, a solution to the auxiliary equations (12)-(13), that we will call a *type-A* solution, is

$$v(x) = \begin{cases} 0, & x \in (-\infty, -\eta], \\ (1 + x/\eta)/2, & x \in [-\eta, \eta] \\ 1, & x \in [\eta, \infty), \end{cases} \quad (17)$$

$$w(x) = \begin{cases} (1 - x/\eta)/2, & x \in [-\eta, \eta], \\ 1, & x \in (-\infty, -\eta], \\ 0, & x \in [\eta, \infty). \end{cases}$$

An example of the type-A solution is displayed in Fig. (1).

We note that there also exists another inner-zone solution to the above leading-order equations $v_{xx} = w_{xx} = 0$, that satisfies b.c. $v(\eta) = -1$, $v(-\eta) = 0$, $w(\eta) = 0$ and $w(-\eta) = -1$:

$$v = -\frac{x}{2\eta} - \frac{1}{2}, \quad w = \frac{x}{2\eta} - \frac{1}{2}. \quad (18)$$

This inner solution is matched to the outer one (15) with the lower sign. In order to make the latter solution also consistent with b.c. (13), we need to connect the two constant solutions $v = \pm 1$ in the outer region $x > \eta$. To this end, we consider a region at $x > \eta$ where $w = 0$ and $g(x) = 1$. Then the second equation in the system (12) is automatically satisfied, and the first equation yields

$$v_{xx} - (a - 1)(v^3 - v) = 0. \quad (19)$$

We choose an arbitrary point $x_0 > 2\eta$ and look for a solution to Eq. (19) in an interval $(x_0 - \eta, x_0 + \eta)$. If $(a - 1)\eta^2 \ll 1$, then the solution is $v = (x - x_0)/\eta$. If $(a - 1)\eta^2 = \mathcal{O}(1)$, then the solution to (19) is $v = \tanh(\sqrt{(a - 1)/2}(x - x_0))$, whose expansion at small $|x - x_0|$ is again $(x -$

$x_0)/\eta$. Thus, to the leading order, an approximate solution to Eqs. (12)-(13) that we call a *type-B* solution, and which is valid for an arbitrary $x_0 > 2\eta$, is

$$v(x) = \begin{cases} 0, & x \in (-\infty, -\eta], \\ -(1 + x/\eta)/2 & x \in [-\eta, \eta], \\ -1, & x \in [\eta, x_0 - \eta], \\ (x - x_0)/\eta, & x \in [x_0 - \eta, x_0 + \eta], \\ 1 & x \in ([x_0 + \eta, \infty). \end{cases} \quad (20)$$

$$w(x) = \begin{cases} 1, & x \in (-\infty, -x_0 - \eta], \\ -(x + x_0)/\eta, & x \in [-x_0 - \eta, -x_0 + \eta], \\ -1, & x \in [-x_0 + \eta, -\eta] \\ (1 - x/\eta)/2, & x \in [-\eta, \eta], \\ 0, & x \in [\eta, \infty). \end{cases}$$

An example of this solution is displayed in Fig 2.

It is easy to see that the type-B solution (20) can also be represented in the form

$$v(x) = 2 f(-x - x_0) - f(-x), \quad w(x) = 2 f(x - x_0) - f(x), \quad (21)$$

where $f(x)$ is the v -component of the type-A solution, i.e.,

$$f(x) \equiv \begin{cases} 0, & x \in (-\infty, -\eta], \\ (1 + x/\eta)/2, & x \in [-\eta, \eta] \\ 1, & x \in [\eta, \infty), \end{cases} \quad (22)$$

The representation (21) suggests that there exists a continuous *family* of solutions to the auxiliary system (12), parametrized by x_0 , so that when $x_0 = 0$, the solution is of the type A, and when $x_0 > 2\epsilon$, the solution is of the type B. In the intermediate case $x_0 \in (0, 2\eta)$, the solution cannot be represented in the simple approximate form (21), and can only be constructed numerically. In other words, the extra kinks in the v - and w - components, which distinguish the solutions of the type B from those of the type A, can be inserted, essentially, at any point, i.e., there is no unique “equilibrium” point at which the extra kinks have to be placed in order to provide for a stationary solution.

Once the general structure of the solutions to the auxiliary system (12) is understood, it is natural to check whether stationary solutions of the underlying equations (8) and (9) follow the same pattern. First, in order to

check the existence of type-A stationary solutions to Eqs. (8) and (9), we have performed numerical integration of the boundary-value problems [8] by means of the finite-difference method in a domain of the size $\Delta x = 100$ (as it will be seen from results displayed below, this size is quite sufficient to consider the system as being practically infinitely large). The number of spatial points was 8192, so that the spatial stepsize was 0.0122.

The numerical problem was thus reduced to a system of algebraic equations of the order $2 \cdot (8192 - 1)$, which were solved by means of the Newton's method with tolerance 10^{-4} . As the first step, we looked for type-A solutions, taking, as initial trials for $v(x)$ and $w(x)$, functions $C/(C + e^{-\gamma x})$ and $C/(C + e^{\gamma x})$ with different values of C and γ , which seem close to the type-A solutions sought for. The calculations have been made over a large range of values of the parameters from Eq. (5), $a = 2 - 1000$ and $\lambda = 0.1 - 10000$. In all cases, a type-A solution has been found indeed.

The next step was to check the existence of the type-B solutions. To this end, we employed two different tests. First, we computed type-B stationary solutions by means of the algorithm described above but with initial trial functions given by the expression (21), where $f(x)$ was replaced by the previously found type-A solution, for the same values of a and λ , and various values of x_0 .

Following this way, in most cases tested we could indeed obtain type-B solutions corresponding to, virtually, arbitrary values of x_0 , in accord with the results of the analysis performed above. However, the result was inconclusive, due to numerical problems, for the most intriguing cases in which x_0 is such that the minima of the initial trial functions (21), with $f(x)$ replaced by the previously found type-A solution, were not close enough to -1 (those values of x_0 are close to 0). In those cases the sequence of approximations produced by the Newton's method did not converge to a solution sought for within the required tolerance in a reasonable amount of steps.

The second method, which, simultaneously, gave a direct information about the dynamical stability of the stationary solutions, was based on simulating the full system of PDEs (8) and (9), this time using the expression (21), with $f(x)$ replaced by the corresponding type-A solution found at the previous step, as an initial configuration. In doing this, we again took different values of the parameter x_0 in Eq. (21).

The numerical simulations of the full nonlinear PDEs were performed using a spectral method with the FFT transform based on 8192 spatial points,

and the modified Euler's method for the time evolution with the step $\delta t = 3 \cdot 10^{-5}$, in a time interval which was checked to be sufficient to obtain a stationary solution (the largest interval was $0 < t < 30$).

The values of x_0 were chosen, in all the cases, as corresponding to $400k$ spatial discretization points, $k = 1, \dots, 6$ (i.e., $x_0 = 4.883, 9.766, 14.648, 19.531, 24.414, 29.297$). We have found that the solution, essentially, remains almost constant in time. In particular, the value of x at which v and w cross zero, while varying from $v = -1$ to $v = 1$ and $w = 1$ to $w = -1$ respectively, remains virtually constant. This numerical observations support the conjecture that the expression (21) with $f(x)$ replaced by the corresponding type-A stationary solution is a fairly good approximation to the type-B solution of Eqs. (6) and (7).

This approximation has been found to further improve as both a and λ in Eq. (5) increase. As an illustration, we show in Fig. 3 the graphs of the v -components of the Type-A and type-B solutions found for $a = 2$ and $\lambda = 10$ at the time moment $t = 30$. The B-type solution was obtained, in accord with what was said above, from the initial condition in the form of Eq. (21) with $f(x)$ replaced by the type-A solution that was found directly from the stationary ODEs.

As well as in the case of the auxiliary system (12) and (14), the existence of the B-type solutions can be qualitatively understood. Indeed, it is clearly seen in Figs. 1 and 2 that the abrupt jump between positive and negative values of, say, v takes place when the w -component is practically equal to zero and, moreover, we may replace $\tanh(\lambda x)$ by $+1$ or -1 , as the above-mentioned jump takes place far from the place where $\tanh(\lambda x)$ is essentially different from ± 1 . Thus, as a matter of fact, we are dealing with a very simple stationary GL equation, (19), about which it is well known that it has a single stable nontrivial solution in the form of a kink, $v = \pm \sqrt{a-1} \tanh\left(\sqrt{(a-1)/2}x\right)$, cf. Eq. (4). Therefore, the jump in the type-B solution exactly corresponds to this kink solution. Moreover, it is known too that more complicated stationary solutions to the real GL equation, containing several kinks and/or antikinks, do not exist, which explains why we have never obtained solutions with a larger number of jumps.

3 Stability of the stationary solutions

Results presented in the previous section suggest that both the type-A and type-B solutions are dynamically stable as stationary solutions to the PDE system. To test the stability in a more systematic way, we simulated the non-stationary equations (6) and (7), adding to the (previously found) stationary solutions small initial perturbations in the form of an arbitrary combination of spatial harmonics compatible with the boundary conditions.

Actually, we, first of all, solved the non-stationary equations (6) and (7) which were linearized around the stationary solutions found in the previous section. In this approximation, all the small perturbations added to an arbitrary type-A stationary solution quickly decay. Thus, we conclude that all these solutions are unequivocally stable.

The situation with the type-B solutions is more tricky: perturbations generally decay, but there remain some residual localized perturbation pulses, which show a clear trend to be stuck exactly at the spots where the jumps of the type-B solution are located, see Fig. 4. The fact that the residual perturbations of the v - and w -components accumulate at the point where, respectively, the v - and w -components of the unperturbed stationary solution make their jumps, is quite easy to understand, as at these points both the v and w fields in the unperturbed solution are nearly equal to zero, hence the nonlinear suppression of the perturbations does not locally take place, allowing the perturbations to survive.

Further simulations, based on the full stationary equations (6) and (7), rather than their linearized versions, demonstrate that, eventually, the residual perturbation pulses seen in Fig. 4(b) decay, but very slowly. This is natural too, as the above-mentioned mechanism disabling the nonlinear suppression of the perturbations is only an approximate one, and it cannot provide for their survival over infinitely long time.

4 Conclusion

In this work, we have introduced a parametrically driven gradient Ginzburg-Landau model, which is subcritical in the absence of the parametric drive. In the case when the parametric drive is uniform in space, a kink solution to this model is stable, on the contrary to the well-known instability of the same

solution in the GL model without the parametric drive. However, a really nontrivial situation takes place when the parametric drive is itself subject to the kink-like spatial modulation, so that it selects real and imaginary constant solutions at $x = \pm\infty$. In this case, we have found stationary solutions numerically, and also analytically for a particular case. The solutions look as being of two different types, viz., a pair of kinks in the real and imaginary components, or the same with an extra kink inserted into each component. We have showed that, in fact, both solutions belong to the same continuous one-parameter family of solutions. Simulations show that the former solution is always stable, while the latter one admits a special type of small perturbations that remain virtually constant in time, rather than decaying or growing. Eventually, these special perturbations decay, but extremely slowly).

We acknowledge valuable discussions with A.A. Nepomnyashchy and W. Zimmermann, and thank Pablo Funes for his help with the software implementation. One of the authors (B.A.M.) appreciates hospitality of the Max Planck Institute for Physics of Complex Systems (Dresden, Germany), where a part of this work was done. H.G.R. acknowledges support from the Fischbach Fellowship.

References

- [1] P. Coulet, J. Lega, and Y. Pomeau, *Europhys. Lett.* **15**, 221 (1991); P. Coulet and K. Emilsson, *Physica D* **61**, 119 (1991).
- [2] I.V. Barashenkov, Yu.S. Smirnov, and N.V. Alexeeva, *Phys. Rev. E* **57**, 2350 (1998); I.V. Barashenkov and E.V. Zemlyanaya, *Phys. Rev. Lett.* **83**, 2568 (1999).
- [3] R.E. Kelly and D. Pal, *J. Fluid Mech.* **86**, 433 (1978); L.P. Vozovoi and A.A. Nepomnyashchy, *Prikl. Mat. Mekh.* **43**, 998 (1979) [English translation: *J. Appl. Math. Mech.* **43**, 1080 (1979)]; G.V. Levina and A.A. Nepomnyashchy, *Prikl. Mat. Mekh* **47**, 402 (1983) [English translation: *J. Appl. Math. Mech.* **47**, 341 (1983)]; P. Coulet and P. Huerre, *Physica D* **23**, 27 (1986).
- [4] D.A.S. Rees and D.S. Riley, *J. Fluid Mech.* **199**, 133 (1989); R. Schmitz and W. Zimmermann, *Phys. Rev. E* **53**, 5993 (1996).
- [5] G. Hartung, F.H. Busse, and I. Rehberg, *Phys. Rev. Lett.* **66**, 2741 (1991).
- [6] B.A. Malomed and A.A. Nepomnyashchy, *Europhys. Lett.* **21**, 195 (1993); *Phys. Lett.* **244**, 92 (1998).
- [7] L. Kramer, E. Ben-Jacob, H. Brand and M.C. Cross, *Phys. Rev. Lett.* **49**, 1891 (1982); Y. Pomeau and S. Zaleski, *J. Phys. (Paris)* **44**, L135 (1983); H. Riecke, *Europhys. Lett.* **2**, 1 (1986); R.B. Hoyle, *Phys. Rev. E* **51**, 310 (1995).
- [8] R.L. Burden and J.D. Faires. *Numerical Analysis* (PWS Publishing Company: Boston, 1980).

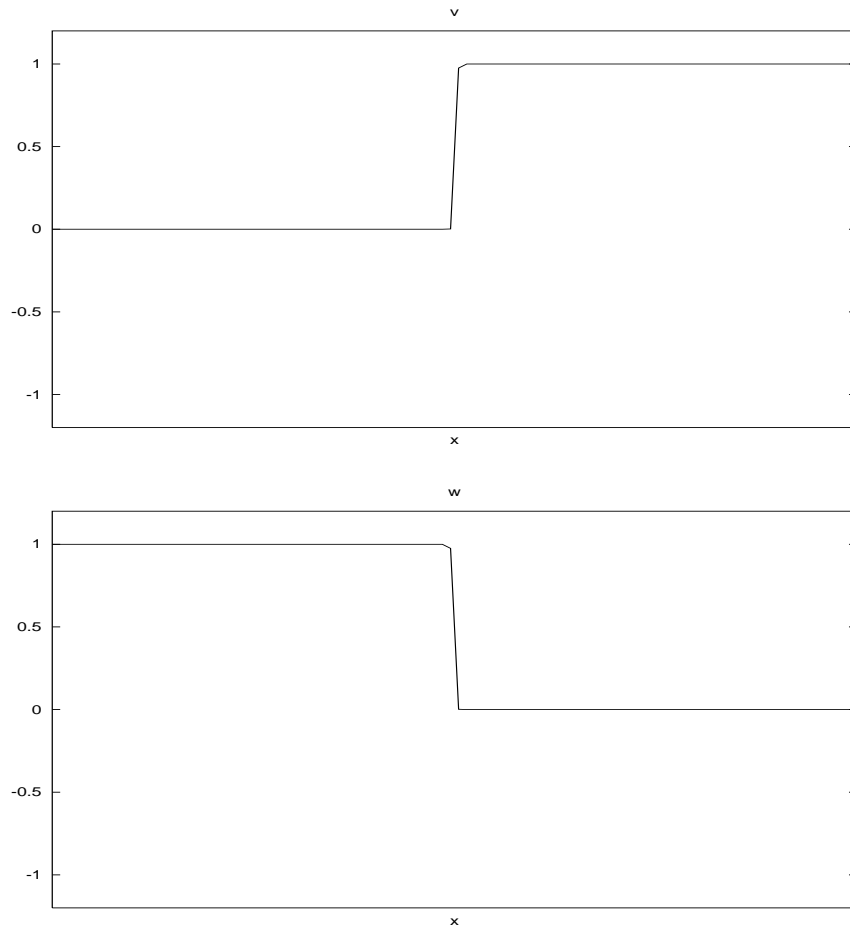


Figure 1: A general scheme of the type-A solution. The corners of the kinks in the v and w components are rounded since the exact solution, unlike the approximation (17), does not admit a discontinuity of the first derivatives.

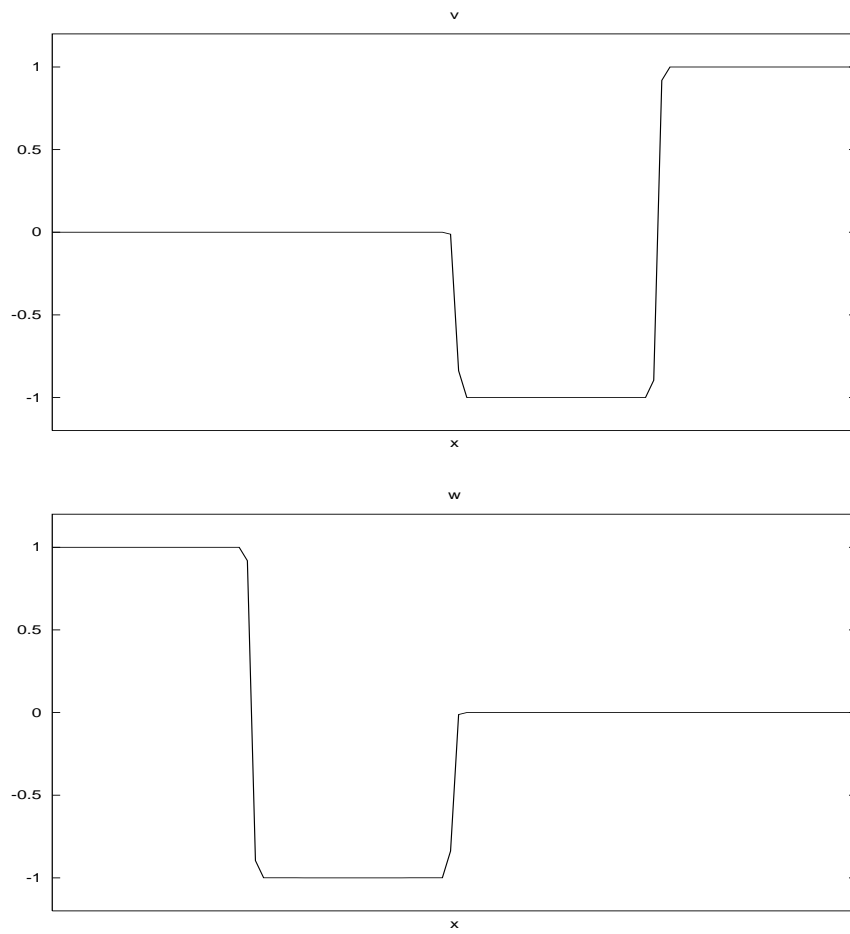


Figure 2: A general scheme of the type-B solution.

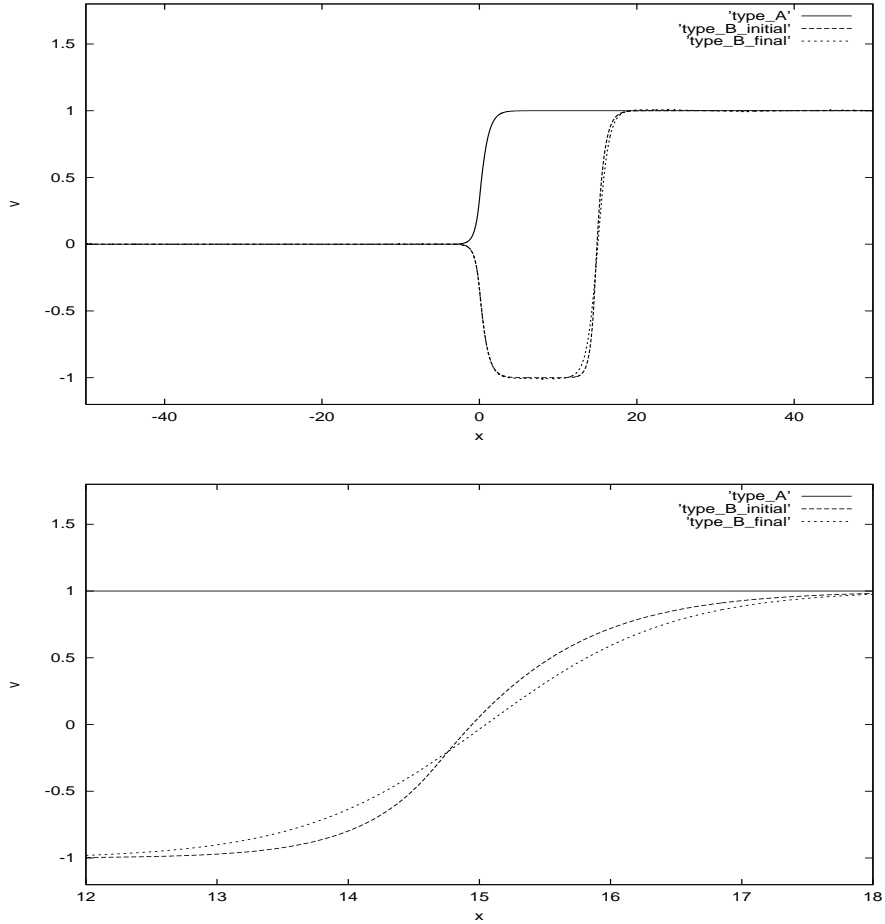


Figure 3: The v - components of the type-A and type-B solutions to Eqs. (8) and (9). The latter solution was obtained using the initial condition in the form (21) with $f(x)$ replaced by the type-A solution, that was found directly from the stationary version of Eqs. (8) and (9). The upper panel displays the solution as a whole, while the lower panel is a blowup of the region where the B-type solution makes its jump. In this figure, $a = 2$, $\lambda = 10$, and the time moment shown is $t = 30$.

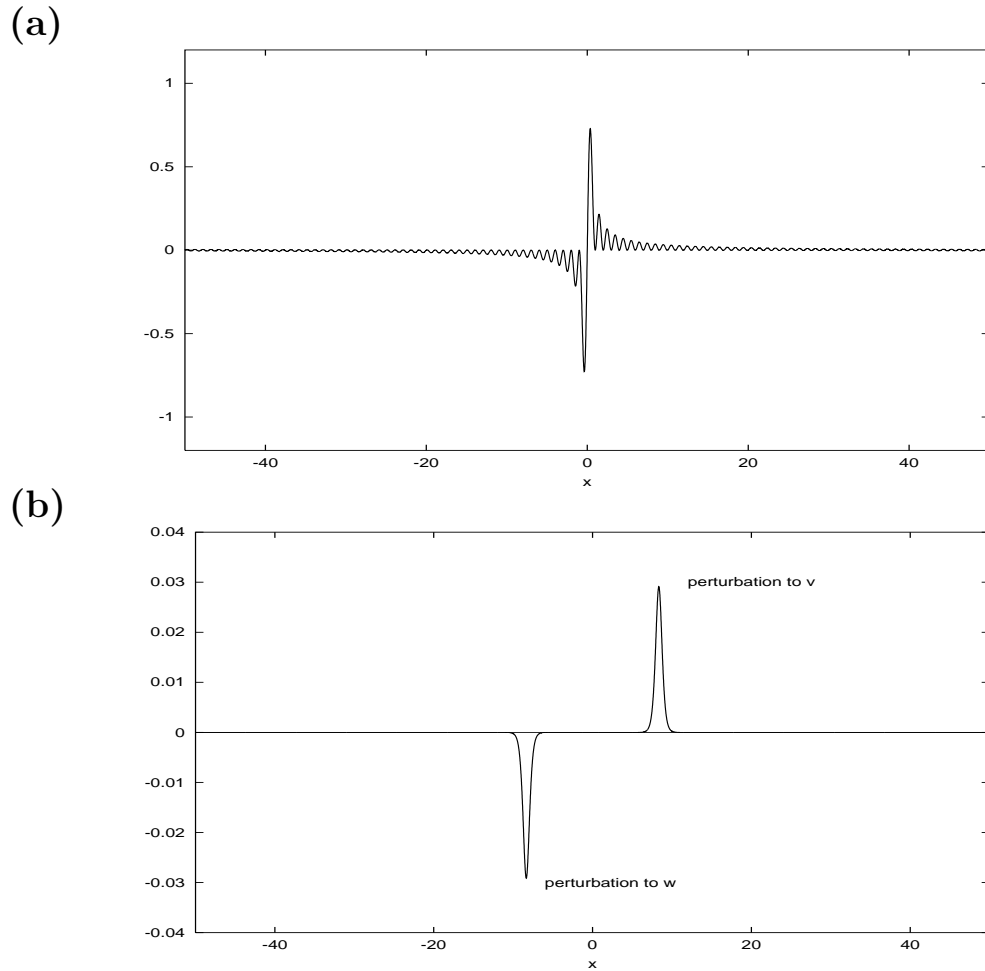


Figure 4: (a) A particular example of the initial perturbation added to the stationary solution of the type B (v - and w -components of this perturbation are equal), that gives rise to practically constant residual perturbation pulses, shown in the panel (b), which are pinned at the points where the type-B solution makes its jump. In this figure, $a = 8.0$, $\lambda = 2.0$, and the panel (b) pertains to the time moment $t = 15$.